

Femtosecond Nanofocusing with Full Optical Waveform Control

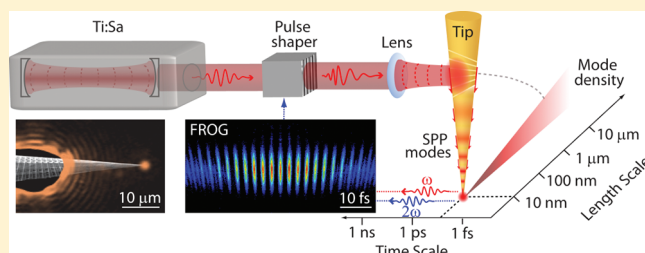
Samuel Berweger,[†] Joanna M. Atkin,[†] Xiaoji G. Xu, Robert L. Olmon, and Markus B. Raschke*

Department of Physics, Department of Chemistry, and JILA, University of Colorado at Boulder, Boulder, Colorado 80309, United States

S Supporting Information

ABSTRACT: The simultaneous nanometer spatial confinement and femtosecond temporal control of an optical excitation has been a long-standing challenge in optics. Previous approaches using surface plasmon polariton (SPP) resonant nanostructures or SPP waveguides have suffered from, for example, mode mismatch, or possible dependence on the phase of the driving laser field to achieve spatial localization. Here we take advantage of the intrinsic phase- and amplitude-independent nanofocusing ability of a conical noble metal tip with weak wavelength dependence over a broad bandwidth to achieve a 10 nm spatially and few-femtosecond temporally confined excitation. In combination with spectral pulse shaping and feedback on the second-harmonic response of the tip apex, we demonstrate deterministic arbitrary optical waveform control. In addition, the high efficiency of the nanofocusing tip provided by the continuous micro- to nanoscale mode transformation opens the door for spectroscopy of elementary optical excitations in matter on their natural length and time scales and enables applications from ultrafast nano-opto-electronics to single molecule quantum coherent control.

KEYWORDS: Nanofocusing, surface plasmon polariton, nonlinear dynamics, nanotip, ultrafast



In order to achieve the goal of an efficient nanometer confined femtosecond light source with independent spatial localization and temporal control of the optical field, and which can freely be manipulated in 3D, the use of the unique properties of surface plasmon polaritons (SPPs) has long been discussed as a potential solution. It is well established that the strong surface field localization and size and shape dependent resonances of SPPs as electromagnetic surface waves associated with collective charge density oscillations at metal–dielectric interfaces allow for subwavelength spatial control of even broadband optical fields.¹ Yet, simple single or coupled nanoparticles as localization and coupling elements suffer from limited power transfer due to the mode mismatch between the propagating incident free-space far-field radiation and the desired nanometer confined SPP excitation volume.²

Elegant solutions to overcome the SPP diffraction limit^{3,4} and achieve nanofocusing based on interference of localized SPP modes exist in the form of specially arranged cascaded, percolated, or self-similar chains of metal nanostructures as optical antennas.^{5–7} In such systems, for suitable spatially distributed and interacting plasmonic geometries with a given overall optical response function $R(\mathbf{r}, t)$, a spatially-, amplitude-, and phase-shaped driving laser field $E(\mathbf{r}, t)$ can result in a specific field localization $E_{\text{loc}}(\mathbf{r}, t')$ in space and time.^{8,9} However, the achievable optical waveforms at the nanofocus are often constrained by the phase relationship between the spectral modes already necessary to achieve the three-dimensional (3D) nanofocusing.¹⁰ This limits the degrees of freedom for full and structurally independent spatial and temporal control of the nanofocused field. Related challenges persist for nanodevices in the form of

tapered grooves, wires, or wedges.^{11–14} While they allow for nanofocusing via their propagating SPP waveguide properties with favorable power transfer, scalability, and broad bandwidth, many such geometries do not allow for full 3D spatial localization independent of spectral phase,^{10,13} and substrate-based designs¹¹ can make spatially and spectrally nondispersive nanofocusing difficult.

In contrast, a 3D tapered tip as an SPP waveguide stands out due to its unique topology as a cone. As has been proposed theoretically,^{15,16} and recently demonstrated experimentally,^{17–19} this geometry allows for true 3D focusing into an excitation volume as small as a few tens of nanometers in size. The divergence of the effective index of refraction with decreasing cone radius experienced by an SPP propagating toward the apex leads to a continuous transformation of cylindrical modes and thus near adiabatic SPP nanofocusing into the apex of the tip. Despite some constraints on power transfer from the propagating SPP to the apex localized excitation due to SPP absorption and reflection, this effect is only weakly wavelength-dependent and the nanofocusing mechanism is expected to be independent of spectral phase.^{20,21}

Here we demonstrate broadband grating coupling and SPP nanofocusing of femtosecond shaped pulses into the apex of an ultrasharp Au tip. Enabled by the phase-independent adiabatic nanofocusing process, full pulse characterization by the nonlinear optical response of the tip allows for not only femtosecond pulse duration optimization but also the generation of arbitrary

Received: July 8, 2011

Revised: August 26, 2011

Published: August 31, 2011

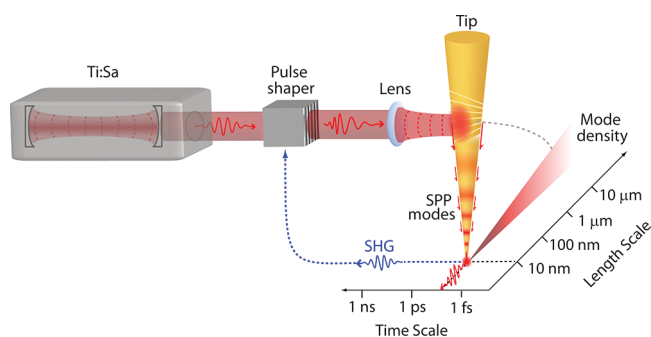


Figure 1. Micro- to nanoscale optical mode transformation on a tip. Broadband SPP coupling of a femtosecond laser pulse onto the shaft of conical Au tip is followed by adiabatic field compression into the nanoscale apex volume. The spatiotemporal coordinate system depicts the associated mode confinement in space and time. The SHG response from the tip is used as feedback for the pulse shaper to optimize pulse duration via MIIPS and to characterize arbitrary optical waveforms in the nanofocus via FROG or XFROG.

ultrafast optical waveforms at the tip apex. Thus we demonstrate the first simultaneous and independent spatiotemporal control of optical fields on nanometer length and femtosecond time scales.

For our experiments, as shown conceptually in Figure 1, we use pulses from a Ti:Sa oscillator with center wavelength ~ 800 nm, bandwidth fwhm ~ 100 nm, nominal pulse duration ~ 10 fs, pulse energy ~ 8 nJ, and repetition rate 75 MHz (Femtolasers Synergy). The pulses are passed through a pulse shaper using a folded 4f geometry with a 640-pixel liquid crystal spatial light modulator (CRI Inc.) for independent spectral amplitude and phase control.²² The beam is focused onto the shaft of electrochemically etched Au tips²³ at 25° incidence using a long working distance objective with NA = 0.35, focal length = 20.5 mm, focus size $\approx 8 \mu\text{m}^2$, and fluence $< 6 \times 10^5 \text{ W/cm}^2$ (Nikon SLWD). A laterally chirped fan-shaped plasmonic grating, cut by focused ion beam milling, enables the launching of broadband propagating SPPs onto the tip where they are concentrated under near-adiabatic conditions into a region tens of nanometers in size at the tip apex and a portion of the fundamental light is re-emitted.^{17,18} In order to provide continuously adjustable nanofocused power a $\lambda/2$ plate is used to change the grating coupling efficiency.

In addition to the emitted fundamental light, the broken axial symmetry at the tip apex allows for the local generation of optical second harmonic (SHG).²⁴ The apex emitted fundamental and SHG light is collected through a separate objective with NA = 0.5 and k-vector direction 90° azimuthal with respect to illumination. The short SPP propagation lengths on Au of $1/\text{Im}(2k_{\text{SPP}}) = 300$ nm at $\lambda = 400$ nm ensures detection of apex-localized emission. The light is then spectrally filtered and detected using a spectrometer with a $\text{N}_2(1)$ -cooled CCD (Princeton Instruments).

Figure 2a shows an SEM image of a tip with a broadband grating superimposed with an optical image showing the far-field illumination incident on the grating and subsequent reradiation of the spatially confined apex SPP field from a region < 25 nm in size, as demonstrated by scanning the tip over a nanometer edged reference sample.¹⁸ The characteristic polarization anisotropy of both the apex-emitted fundamental and localized SHG show the expected $\cos^2(\theta)$ intensity dependence expected for a point dipole emitter. Note the different fundamental grating input polarization dependencies with $\cos^2(\theta)$ dependence on

fundamental apex emission, and $\cos^4(\theta)$ dependence for SHG emission. Typically, for ~ 30 mW incident light on the grating we estimate the total apex emission to be $\sim 100 \mu\text{W}$ fundamental and ~ 10 pW SHG.

After optimizing the grating illumination and coupling parameters for maximum coupling bandwidth or SHG intensity depending on application, the optical waveform of the nanofocus is controlled using spectral pulse shaping with SHG as the feedback parameter for the multiphoton intrapulse interference phase scan (MIIPS) algorithm used.²⁵ The MIIPS-optimized pulses are then characterized via interferometric frequency resolved optical gating (IFROG)^{26,27} and the transient is reconstructed with phase and amplitude information from the DC portion of the spectrogram using a standard FROG retrieval algorithm. In order to obtain reliable IFROG measurements identical grating coupling conditions for both pulse replicas must be ensured. This can be accomplished using the pulse shaper to generate perfectly collinear pulse pairs with the applied mask $M(\omega)$

$$M(\omega) = \cos(\phi(\omega)/2)e^{i\phi(\omega)/2} \quad (1)$$

with carrier frequency ω and spectral phase ϕ , where or

$$\phi(\omega) = \phi_0 + \phi_1(\omega - \omega_0) + \frac{\phi_2}{2!}(\omega - \omega_0)^2 + \dots \quad (2)$$

resulting in two pulse replica one of which is delayed in time by ϕ_1 .²⁸ Furthermore, with the capability to generate arbitrary (limited only by resolution of the spatial light modulator) relative n th order spectral phase (dispersion) ϕ_n between the pulses, interferometric cross-correlation (XFROG) measurements can also be performed.

Figure 3a shows an IFROG trace for few-femtosecond broadband nanofocusing with corresponding reconstructed spectral (Figure 3b) and temporal (Figure 3c) intensity profiles (red) and phase (blue). After MIIPS optimized flattening of the spectral phase to within 0.1 rad within the primary portion of the pulse, we obtain a transform-limited pulse with a duration of ≈ 16 fs for the given coupling bandwidth of fwhm ≈ 60 nm in this case. The result is shown in Figure 3c along with the temporal electric field transient obtained (green).

To demonstrate the capability to nanofocus a femtosecond pulse of arbitrary waveform, we generate a chirped pulse with a group delay dispersion of $\phi_2 = 200 \text{ fs}^2$ at the tip apex as an example. Figure 4a shows the measured XFROG trace using a transform limited 16 fs pulse with identical spectrum as reference. Figure 4b shows the associated temporal variation in instantaneous carrier wavelength. The reconstructed spectral intensity of the chirped pulse is shown in Figure 4c (red). The comparison and good agreement between the reconstructed phase (solid blue) and the applied phase function of $\phi_2 = 200 \text{ fs}^2$ (black dashed) as set by the pulse shaper show the high degree of accuracy of this procedure. Shown in Figure 4d are the corresponding time-domain intensity (red), phase (blue), and electric field transient (green) with the shift in the instantaneous frequency indicated across the chirped pulse.

These two examples demonstrate the unique ability of the 3D tapered tip for simultaneous SPP nanofocusing and optical waveform control compared to the alternative geometries and approaches mentioned above. By relying on the diverging index of refraction experienced by propagating SPPs with decreasing cone radius, the mode transformation into a nanoscale excitation at the tip apex remains continuous and impedance matched,¹⁶ while the uniform taper surface prevents the otherwise typical

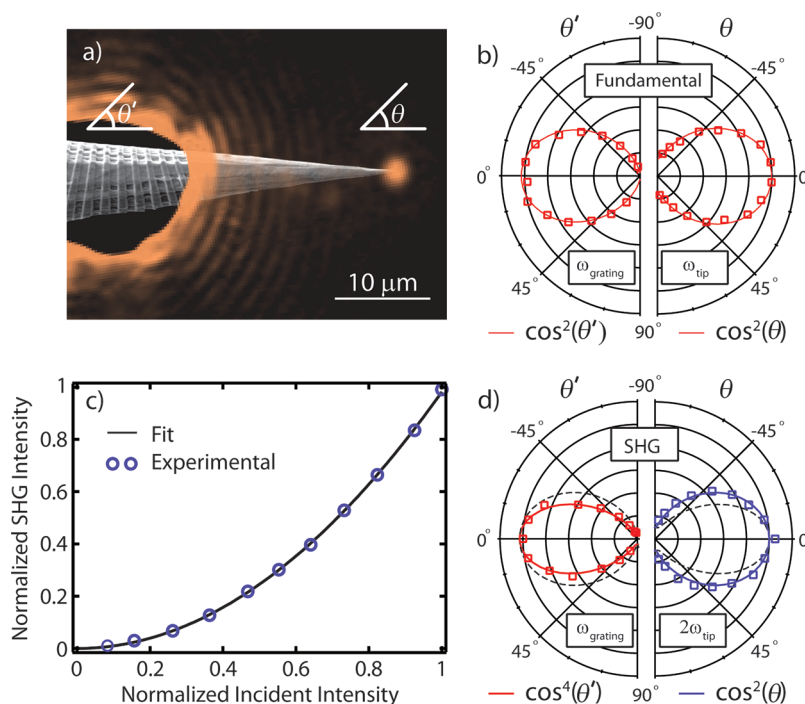


Figure 2. Broadband tip nanofocusing and intrinsic nonlinear response: Optical image (a) of the grating coupled and apex emitted light superimposed with an SEM image of the tip with a broadband laterally chirped fan-shaped grating. Polarization anisotropy (b) of the grating coupled and apex-emitted fundamental light, demonstrating the $\cos^2(\theta)$ dependence expected of a point dipole at the apex, oriented parallel to the tip axis.¹⁸ Intensity dependence (c) of the apex emitted SHG on the incident light (blue circles) and a $I(2\omega) \propto I(\omega)^2$ fit (black line). Polarization anisotropy (d) of the apex emitted SHG, exhibiting a $\cos^2(\theta)$ dependent emission, and a $\cos^4(\theta')$ dependence on the grating incident fundamental polarization.

scattering and reflection losses at structural discontinuities. Because of the radial symmetry and decreasing SPP group velocity, full nanoconfinement in all spatial dimensions is achieved.^{18,19,29}

While the size of the emitter is largely established by the dimension of the tip apex, the effective nanofocus size as relevant for imaging applications is determined by the spatial extent of the evanescent field of the apex, given by the magnitude of the surface-normal imaginary SPP k -vector. A resolution as small as 7 nm has been previously determined.^{18,19,30} In principle for very sharp tips, at least within the limits set by skin depth and finite size effects of the dielectric function, focusing down to just a few nanometers would be conceivable.

In addition to providing spatial confinement, the tips allow for the desired broadband excitation necessary for true femtosecond optical control. As predicted theoretically, the nanofocusing efficiency is maximal in the 800 nm range for a tip cone angle of $\sim 14^\circ$ ^{20,31} as used in our experiment with previously demonstrated monochromatic nanofocusing efficiencies of up to 9%.²⁹ Since the SPP nanofocusing mechanism does not rely on localized SPP resonance conditions, its weak wavelength dependence provides phase-independent nanofocusing over a broad wavelength range as desired for ultrafast pulses as short as just a few femtoseconds.²⁰ As a direct consequence, the spectral phase and amplitude of the coupled pulse are retained as degrees of freedom that can be controlled independently.

In contrast to other nanofocusing structures based either on localized plasmon resonances⁵ or propagating SPP modes^{10,13} that exhibit a dependence of the spatial localization on the spectral and phase characteristics of the excitation field, we control the pulse duration and optical waveform at the tip

apex via deterministic pulse shaping, as opposed to adaptive techniques,³² thus reducing the computation duration of the optimization procedure as well as algorithm complexity. Furthermore, in order to characterize the designed nanofocus waveform both in terms of spectral phase and amplitude, the nanofocused apex field conveniently generates local SHG. This structurally intrinsic coherent nonlinear response thus enables a direct means to apply appropriate spectrogram-based nonlinear wavemixing pulse characterization techniques (e.g., FROG, XFROG) for the complete optical waveform determination and optimization without the requirement for a separate nonlinear material or asymmetric structure for nonlinear optical frequency conversion.

The theoretical limit for the shortest attainable pulse duration at the tip apex is determined only by the coupling bandwidth³³ and the dephasing time T_2 in the case of spectral overlap with a localized SPP of the tip apex.³⁴ While the tips used in our off-resonant experiments shown here typically exhibit SPP resonances in the vicinity of 650 nm, the use of localized tip SPPs with measured dephasing times of up to $T_2 \approx 20$ fs²⁶ can provide additional capability for tailoring the optical waveform with higher field enhancement, albeit at the expense of minimal pulse duration.

The details of the nanofocusing mechanism and the degree of adiabaticity are not yet completely understood as the optimal nanofocusing conditions require minimization of both SPP propagation damping and reflection losses, which increase and decrease with adiabatic conditions, respectively. This includes the propagation induced group delay dispersion (GDD) which is of particular interest for femtosecond nanofocusing. However, considering a group velocity dispersion of $\partial^2 k / \partial \omega^2 \approx 0.4$ fs²/μm for an SPP propagating on a flat surface, the dispersion

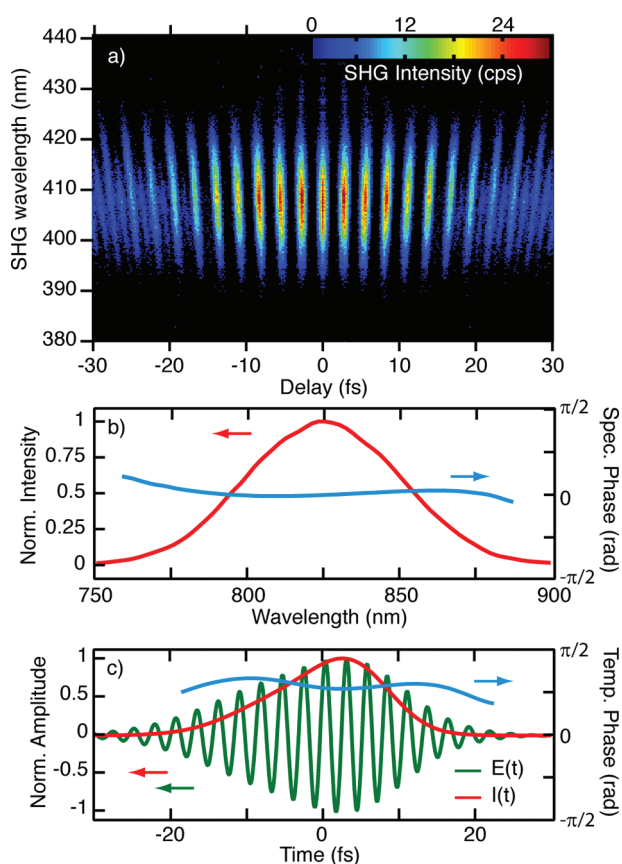


Figure 3. Nanofocusing of a few femtosecond pulse at the tip: FROG measurement based on apex localized SHG (a) of adiabatically nano-focused SPP. MIIPS optimization for flat spectral phase yields a nearly transform limited 16 fs pulse for a 60 nm fwhm bandwidth (b and c) with reconstructed spectral and temporal phase (blue), intensity (red), as well as the reconstructed temporal electric field transient (green).

introduced by a propagation length of 20 μm would be expected to be small. This is in good agreement with comparison of grating-coupled and free-space MIIPS measurements showing little GDD introduced by grating-coupling and subsequent SPP nanofocusing waveguide dispersion, although some tip-to-tip variability is observed. While arbitrary group delay dispersion could be compensated within the capability of the pulse shaper using MIIPS, the apparent low dispersion provides favorable conditions for pulse optimization and characterization by yielding already large initial SHG levels.

The use of a grating as coupling element can provide high coupling efficiencies, but some scattering losses are inevitable. The fan-shaped gratings developed for this work enable a high coupling bandwidth with fwhm of up to ~ 100 nm (see Supporting Information). Improvements in the form of grating structures with optimized groove depth and holographic geometries, chirped gratings including Bragg reflectors,³⁵ broadband coupling via fabricated micropillar onto the tip shaft,³⁶ spatial pulse shaping in the far-field excitation focus,³⁷ and tip fabrication with reduced surface roughness could further improve the tip performance for nanofocus optical waveform control. Without the need for resonance behavior in order for spatial localization to occur, the process can be extended to a wide range of wavelengths, limited in principle only by material damping at short

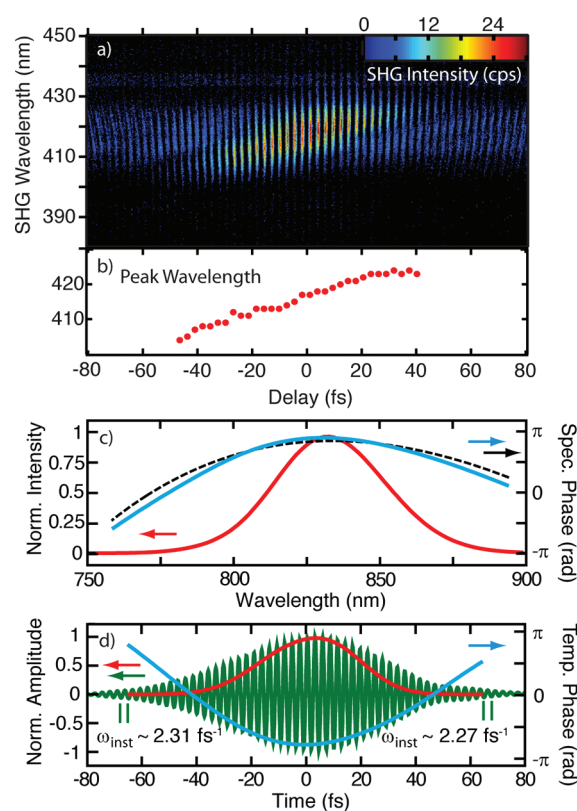


Figure 4. Deterministic arbitrary optical waveform control at the nanofocus: Interferometric XFROG measurement of the apex field with an applied group delay dispersion of 200 fs^2 with a transform limited 16 fs pulse as reference (a), with corresponding temporal variation in XFROG peak wavelength (b). Reconstructed spectral characteristics (c) of the chirped pulse with intensity (red), and spectral phase (blue) in comparison with the theoretical 200 fs^2 GDD applied (dashed). Reconstructed chirped electric field transient (green) (d).

wavelengths, and taper angle and reduced spatial field confinement at long wavelengths.

In summary, we have demonstrated independent nanometer spatial and femtosecond temporal optical waveform control, enabled by nanoscale field concentration via adiabatic SPP nanofocusing into monolithic gold tips, which is intrinsically broadband and independent of the instantaneous frequency and spectral phase of the excitation field. The in-principle impedance matched far-field to near-field mode transformation allows for efficient power transfer into a nanoconfined volume at the tip apex. This light source with arbitrary waveform control at the nanoscale is of a fundamentally new quality compared to both conventional far- and near-field sources. It allows for the systematic extension of near background-free scanning probe microscopy^{19,29,30} to the nanoscale implementation of many forms of nonlinear and ultrafast spectroscopies for spatiotemporal imaging.^{38–40} This offers all-optical access to the study of nonequilibrium carrier and lattice excitations and their correlations on the level of their natural femtosecond time and nanometer length scales, thus providing unprecedented microscopic insight into the origin of complex biological, organic, or correlated electron materials. It allows for quantum coherent control of chemical reactions⁴¹ on the nanoscale, quantum information processing, provides a tool for nanophotonic circuit analysis, and, with the high field compression, new avenues for

extreme nonlinear optics such as higher harmonic generation^{42,43} or femtosecond electron pulse generation.⁴⁴

■ ASSOCIATED CONTENT

S Supporting Information. Additional information and figure. This material is available free of charge via the Internet at <http://pubs.acs.org>.

■ AUTHOR INFORMATION

Corresponding Author

*E-mail: markus.raschke@colorado.edu.

Author Contributions

[†]These authors contributed equally to this work

■ ACKNOWLEDGMENT

We would like to acknowledge valuable discussions with Mark Stockman, Christoph Lienau, Steve Cundiff, and Hrvoje Petek as well as funding from the National Science Foundation (NSF CAREER Grant CHE 0748226). Part of the work was performed at the Environmental Molecular Sciences Laboratory (EMSL), a national scientific user facility from DOE's Office of Biological and Environmental Research at Pacific Northwest National Laboratory (PNNL). PNNL is operated by Battelle for the US DOE under the contract DEAC06-76RL01830.

■ REFERENCES

- (1) Schuller, J. A.; Barnard, E. S.; Cai, W.; Jun, Y. C.; White, J. S.; Brongersma, M. L. *Nat. Mater.* **2010**, *9*, 193.
- (2) Schuck, P. J.; Fromm, D. P.; Sundaramurthy, A.; Kino, G. S.; Moerner, W. E. *Phys. Rev. Lett.* **2005**, *94*, 017402.
- (3) Yin, L.; Vlasko-Vlasov, V. K.; Pearson, J.; Hiller, J. M.; Hua, J.; Welp, U.; Brown, D. E.; Kimball, C. W. *Nano Lett.* **2005**, *5*, 1399.
- (4) Liu, Z.; Steele, J. M.; Srituravanich, W.; Pikus, Y.; Sun, C.; Zhang, X. *Nano Lett.* **2005**, *5*, 1726.
- (5) Aeschlimann, M.; Bauer, M.; Bayer, D.; Brixner, T.; Cunovic, S.; Dimler, F.; Fischer, A.; Pfeiffer, W.; Rohmer, M.; Schneider, C.; Steeb, F.; Strüber, C.; Voronine, D. V. *Proc. Nat. Acad. Sci. U.S.A.* **2010**, *107*, 5329.
- (6) Gunn, J. M.; High, S. H.; Lozovoy, V. V.; Dantus, M. J. *Phys. Chem. C* **2010**, *114*, 12375.
- (7) Li, K.; Stockman, M. I.; Bergman, D. J. *Phys. Rev. Lett.* **2003**, *91*, 227402.
- (8) Volpe, G.; Molina-Terriza, G.; Quidant, R. *Phys. Rev. Lett.* **2010**, *105*, 216802.
- (9) Stockman, M. I.; Faleev, S. V.; Bergman, D. J. *Phys. Rev. Lett.* **2002**, *88*, 067402.
- (10) Durach, M.; Rusina, A.; Stockman, M. I.; Nelson, K. *Nano Lett.* **2007**, *7*, 3145.
- (11) Volkov, V. S.; Bozhevolnyi, S. I.; Rodrigo, S. G.; Martin-Moreno, L.; Garcia-Vidal, F. J.; Devaux, E.; Ebbesen, T. W. *Nano Lett.* **2009**, *9*, 1278.
- (12) Fang, Y.; Fei, H.; Hao, F.; Nordlander, P.; Xu, H. *Nano Lett.* **2009**, *9*, 2049.
- (13) Cao, L.; Nome, R. A.; Montgomery, J. M.; Gray, S. K.; Scherer, N. F. *Nano Lett.* **2010**, *10*, 3389.
- (14) Verhagen, E.; Spasenovic, M.; Polman, A.; (Kobus) Kuipers, L. *Phys. Rev. Lett.* **2009**, *102*, 203904.
- (15) Babadjanyan, A. J.; Margaryan, N. L.; Nerkararyan, K. V. *J. Appl. Phys.* **2000**, *87*, 3785.
- (16) Stockman, M. I. *Phys. Rev. Lett.* **2004**, *93*, 137404.
- (17) Ropers, C.; Neacsu, C.; Elsaesser, T.; Albrecht, M.; Raschke, M.; Lienau, C. *Nano Lett.* **2007**, *7*, 2784.
- (18) Neacsu, C. C.; Berweger, S.; Olmon, R. L.; Saraf, L. V.; Ropers, C.; Raschke, M. B. *Nano Lett.* **2010**, *10*, 592.
- (19) Sadiq, D.; Shirdel, J.; Lee, J. S.; Selishcheva, E.; Park, N.; Lienau, C. *Nano Lett.* **2011**, *11*, 1609.
- (20) Issa, N.; Guckenberger, R. *Plasmonics* **2007**, *2*, 31.
- (21) Gramotnev, D. K.; Vogel, M. W.; Stockman, M. I. *J. Appl. Phys.* **2008**, *104*, 034311.
- (22) Weiner, A. M. *Rev. Sci. Instrum.* **2000**, *71*, 1929.
- (23) Ren, B.; Picardi, G.; Pettinger, B. *Rev. Sci. Instrum.* **2004**, *75*, 837.
- (24) Neacsu, C. C.; Reider, G. A.; Raschke, M. B. *Phys. Rev. B* **2005**, *71*, 201402.
- (25) Xu, B.; Gunn, J. M.; Dela Cruz, J. M.; Lozovoy, V. V.; Dantus, M. J. *Opt. Soc. Am. B* **2006**, *4*, 750.
- (26) Anderson, A.; Deryckx, K. S.; Xu, X. G.; Steinmeyer, G.; Raschke, M. B. *Nano Lett.* **2010**, *10*, 2519.
- (27) Trebino, R.; DeLong, K. W.; Fittinghoff, D. N.; Sweetser, J. N.; Krumbügel, M. A.; Richman, B. A.; Kane, D. J. *Rev. Sci. Instrum.* **1997**, *68*, 3277.
- (28) Shim, S. H.; Zanni, M. T. *Phys. Chem. Chem. Phys.* **2009**, *11*, 737.
- (29) Berweger, S.; Atkin, J. M.; Olmon, R. L.; Raschke, M. B. *J. Phys. Chem. Lett.* **2010**, *1*, 3427.
- (30) De Angelis, F.; Das, G.; Candeloro, P.; Patrini, M.; Galli, M.; Bek, A.; Lazzarino, M.; Maksimov, I.; Liberale, C.; Andreani, L. C.; Di Fabrizio, E. *Nat. Nanotechnol.* **2009**, *5*, 67.
- (31) Baida, F.; Belkhir, A. *Plasmonics* **2009**, *4*, 51.
- (32) Aeschlimann, M.; Bauer, M.; Bayer, D.; Brixner, T.; Garcia de Abajo, F. J.; Pfeiffer, W.; Rohmer, M.; Spindler, C.; Steeb, F. *Nature* **2007**, *446*, 301.
- (33) Sadiq, D.; Shirdel, J.; Vasa, P., and Lienau, C., *Proceedings of the 5th International Conference on Surface Plasmon Photonics*, Busan, Korea; May 15-20, 2011 and private communication with C. Lienau.
- (34) Sönnichsen, C.; Franzl, T.; Wilk, T.; von Plessen, G.; Feldmann, J.; Wilson, O.; Mulvaney, P. *Phys. Rev. Lett.* **2002**, *88*, 077402.
- (35) Lopez-Tejeira, F.; S. R. R.; Martin-Moreno, L.; Garcia-Vidal, F. J.; Devaux, E.; Ebbesen, T. W.; Krenn, J. R.; Radko, I. P.; Bozhevolnyi, S. I.; Gonzalez, M. U.; Weeber, J. C.; Dereux, A. *Nat. Phys.* **2007**, *3*, 324.
- (36) Sánchez, E. J.; Krug, J. T., II; Xie, X. S. *Rev. Sci. Instrum.* **2002**, *73*, 3901.
- (37) Piestun, R.; Miller, D. A. B. *Opt. Lett.* **2001**, *26*, 1373.
- (38) Terada, Y.; Yoshida, S.; Takeuchi, O.; Shigekawa, H. *Nat. Photonics* **2010**, *4*, 869.
- (39) Kubo, A.; Onda, K.; Petek, H.; Sun, Z.; Jung, Y. S.; Kim, H. K. *Nano Lett.* **2005**, *5*, 1123.
- (40) Brixner, T.; de Abajo, F. J. G.; Schneider, J.; Pfeiffer, W. *Phys. Rev. Lett.* **2005**, *95*, 093901.
- (41) Assion, A.; Baumert, T.; Bergt, M.; Brixner, T.; Kiefer, B.; Seyfried, V.; Strehle, M.; Gerber, G. *Science* **1998**, *282*, 919.
- (42) Bartels, R.; Backus, S.; Zeek, E.; Misoguti, L.; Vdovin, G.; Christov, I. P.; Murnane, M. M.; Kapteyn, H. C. *Nature* **2000**, *406*, 164.
- (43) Kim, S.; Jin, J.; Kim, Y. J.; Park, I.-Y.; Kim, Y.; Kim, S. W. *Nature* **2008**, *453*, 757.
- (44) Ropers, C.; Solli, D. R.; Schulz, C. P.; Lienau, C.; Elsaesser, T. *Phys. Rev. Lett.* **2007**, *98*, 043907.